Available online at www.sciencedirect.com

ScienceDirect

materialstoday: PROCEEDINGS

[*Recent Trends in Environment and Sustainable Development (RTESD-2019): Materials Science*]

Cu clusters modified aligned titania nanotubes for photoelectrochemical water splitting

Preetam K. Sharma*, Jeremy W. J. Hamilton, J. Anthony Byrne

NIBEC, Ulster University, Shore Road, Newtownabbey, BT37 0QB, United Kingdom
**pk.sharma@ulster.ac.uk*

Abstract

Limited availability of the fossil fuel resources, and their environmental impact has led to a rapid increase in the scientific interest towards renewable energy sources. Photoelectrochemical water splitting to produce hydrogen is one such technology. In the current work, aligned titania nanotubes were fabricated by electrochemical anodization and surface engineered with sub-nanometer Cu clusters for the enhanced photoelectrochemical responses. The nanotubes have anatase crystalline structure and are well covered on the surface as shown by using X-ray diffraction and scanning electron microscopy. The surface modification of the nanotubes using Cu clusters enhanced the photoelectrochemical responses, indicative of improving the water splitting yield. The enhancement in photocurrent could be explained due to an extended absorption range or reduced recombination. As the enhancement was limited to the UV region and no visible response was observed it was considered unlikely the surface modification altered the materials band gap. Instead, the enhancement is considered to be due to reduced recombination.

Keywords: Titania nanotubes; Cu clusters; surface engineering; materials characterisation; photoelectrochemical response

1. Introduction

In photocatalysis processes, a semiconductor is irradiated with the photons of higher energy than band-gap ($h\upsilon > E_g$), and electron-hole pairs are generated which take part in the secondary reactions at the surface. Photocatalytic energy harvesting by utilising the generated charge carriers for water splitting or CO_2 reduction to generate fuels can be an attractive alternative to fossil fuels [1]. TiO_2 is one of the most investigated photocatalytic material owning to its high stability and excellent UV activity [2]. Titanium dioxide is naturally present in three crystalline structures namely anatase, rutile and brookite [3]. Out of all available polymorphs, anatase is the most investigated due to its higher photoactivity [4].

Several approaches have been utilised for the enhancement of the photocatalytic activity of TiO_2. These include optimizing the crystalline structure (facet engineering or anatase-rutile mixed phases), novel morphologies, fabricating heterojunctions, doping and surface engineering [5]. A multi aspect approach of creating a heterostructure on the surface of a novel TiO_2 morphology via partially oxidised metallic clusters as surface modifiers is taken in this investigation. A number of nanostructured TiO_2 morphologies including nanoparticles, thin films, nanowires, nanorods and nanotubes have been investigated in past [6]. Out of these, self-aligned titania nanotubes are an attractive option. Titania nanotubes are easy to fabricate and are reported to show excellent photoelectrochemical response due to higher surface area, higher photon absorption and lower defects [7].

Metallic and semiconductor cluster (<2 nm particles) modified materials have been prepared in past directly on the

parent photocatalyst by chemisorption calcination cycles [8], photo-deposition from salts [9] or by vacuum deposition techniques. In many of these techniques, the average size and distribution of cluster size can be difficult to control. These problems arise as cluster growth relies on a seeding effect from which larger clusters are grown. On anisotropic defective materials, such as nanoparticle surfaces, preferential deposition at defect sites can occur. Here, the surface modifying cluster is synthesised and stabilised separately to allow greater control of particle size distribution before subsequent attachment to the host material whereby localisation by the surface seeding effect can be avoided. The use of Cu modified TiO_2 photocatalysts have been reported as a successful strategy for improving photocatalytic water splitting and CO_2 reduction activity [10,11].

In the current work, TiNTs have been modified with sub-nanometer Cu clusters. The prepared materials were characterised and investigated for the photoelectrochemical water splitting. Standardisation in photocatalysis research is a big concern and comparing results from different groups is not easy and sometimes impossible due to variation is electrodes, set-up and irradiation source. The current work helps in direct comparison of Cu clusters on two different TiO_2 nanostructures, namely P25 and TiNTs in similar conditions [12].

2. Experimental section

2.1. Synthesis of copper clusters

Cu clusters were synthesized by adopting a modified Brust-Schiffrin protocol, reported elsewhere [12]. In brief, $Cu(NO_3)_2.3H_2O$ and tetra-n-octylammonium bromide (TOAB) were dissolved in absolute ethanol under constant stirring. The solution was held at 80°C for 30 min followed by cooling using ice water jacket. After cooling, Ar was bubbled through the solution and 2-mercapto-5-n-propylpyrimidine (C_3H_7-$C_4N_2H_2$-SH) was added. The solution was reacted for 12 h. Reducing agent, $NaBH_4$ in ethanol was then added to the reaction mixture. The reaction was kept on for another 7 h before centrifugation to recover the pellet. The pellet was washed with ethanol and centrifuged again. The final pellet was dried and turned to powder using mortar-pestle.

2.2. Fabrication of aligned titania nanotubes

Ti foil samples (30 x 60 mm^2) were cleaned before anodization. The foils were sonicated then washed multiple times in 5% detergent solution, distilled water and ethanol, sequentially followed by drying under a stream of Ar. The Ti foil was anodised in a custom-built electrochemical cell with Ti foil as the anode and Pt as the cathode. For the preparation of the electrolyte, 0.3 wt.% NH_4F and 3.0% distilled water were dissolved in 97 vol% ethylene glycol solution [13]. The electrochemical anodization was performed for 3 h at 30 V. The anodised foils were washed multiple times in distilled water. Finally, the foils were annealed in air at 500˚C for 20 h (2 ˚C ramp up and 1 ˚C ramp down).

2.3. Electrode preparation

Considering the square packing, 80% TiNTs coverage on Ti foil and 10% spray-coating yield, the loading of copper was calculated. The nanotubes length, inner and outer diameter of 1200 nm, 18 nm and 60 nm respectively, the average from TEM measurements, were used for the calculation of Copper modifier. The loading of Cu on the surface of nanotubes was estimated to get an approximate monolayer coverage on the surface of the nanotubes. For the preparation of Cu-TiNTs, 250 µg cm^{-2} Cu clusters (corresponding to the Ti foil area) in methanol were sonicated. The sonicated solution was spray coated on the annealed TiNTs substrate followed by annealing at 550 ˚C for 1 h (ramp $2^oC\ min^{-1}$ up, $1^oC\ min^{-1}$ down).

Foils were connected to a Cu wire by using conductive silver epoxy (Circuitworks CW2400) and the assembly coated in SU8 photoresist (MicroChem) to insulate the entire electrode except an active area of 30 x 30 mm^2. The photoresist was fixed by exposing to UVB for 5 min on both sides followed by hard baking at 160°C.

For optimising the loading of Cu on titania, titania films were grown on Ti foil by annealing at 550°C for 1 h (ramp $2^oC\ min^{-1}$ up, $1^oC\ min^{-1}$ down). The annealed films were loaded with Cu clusters, the loading was similar to the loading on the titania nanotubes. Two higher loadings of Cu (5x and 20x) were also investigated.

2.4. Photoelectrochemical measurements

An electrochemical workstation coupled with a custom-built photoelectrochemical cell. The cell has a quartz window for allowing UV and visible photons to be irradiated on the electrode surface. Xe lamp (450 W) was used as the irradiation source. The total UV irradiance of the lamp was 16.6 W m^{-2} nm^{-1} which is approximately one third of AM 1.5 (ASTM NREL data). The effective irradiated area was 1.0*1.1 cm^2. UV cut-off filters were used to give polychromatic visible only irradiation studies (λ > 435 nm; 10 nm FWHM), while a monochromator was used to give a narrow band of irradiation to measure the spectral response. A mechanical chopper was used for chopped irradiation experiments. The measurements were performed in a three-electrode configuration, where Pt gauze and saturated calomel electrodes were used as counter and reference electrodes, respectively. 0.1 M $HClO_4$ was used as supporting electrolyte. Linear sweep voltammetry (LSV) measurements were performed under polychromatic irradiation (full spectrum) or visible (λ > 435 nm) to measure the photocurrent-potential response. The irradiation was chopped to give light on/light off at a frequency of 10 s. The sweep rate was 5 mVs^{-1}, sweeping from -1.0 V to +1.0 V. The photocurrent spectral response was measured at fixed potential of 0.5 V under monochromatic irradiation, increasing the wavelength at the intervals of 10 nm in the dark cycle.
The photocurrent action spectra were used to determine the incident photon-to-current conversion efficiency (IPCE). IPCE is given in equations 1 and 2 [14]:

$$\text{IPCE} = \frac{\text{number of electron}-\text{hole pairs generated}}{\text{number of incident photons}} \qquad \text{(eq. 1)}$$

$$\text{or,} \qquad \text{IPCE (\%)} = \frac{hc}{e}\left(\frac{j_{photo}(\lambda)}{\lambda P(\lambda)}\right) * 100 \qquad \text{(eq. 2)}$$

2.5. Materials Characterisation

The aligned nanotubes were scraped off from the Ti foil in ethanol solution. The scraped TiNTs were sonicated in ethanol followed by drop-casting on the TEM grid to determine the wall thickness as well as the length of the nanotubes. Transmission electron microscopy (TEM) images and selected area electron diffraction (SAED) were recorded on JEOL JEM-2100F microscope at 200 kV bias voltage. Scanning transmission electron microscopy (STEM) measurements were performed on the JEOL instrument using Gatan high-angle annular dark field (HAADF) and JEOL bight field (BF) detectors. Scanning electron microscopy (SEM) images were recorded using Hitachi SU5000 field emission SEM at 10 kV. X-ray diffractograms (XRD) were recorded on Bruker D8 Discover in 20 - 80˚ range.

3. Results and discussion

3.1. Characterisation results

Fig. 1 shows the (a) SEM image and (b) XRD of the nanotubes on the surface of the Ti foil. The nanotubes are evenly distributed on the surface of the foil as seen from SEM. The average inner and outer diameter of the nanotubes, measured using SEM, are 65.5 nm and 90 nm, respectively. The obtained XRD was compared to JCPDS card no. 21-1272 standard. From the Fig. (b), TiNTs show A(101) and A(004) as dominant peaks. This confirms that the nanotubes have anatase crystalline structure. Additional peaks from Ti metal, which is underneath the nanotubes, were also observed. The XRD analysis of the Cu clusters and Cu-TiNTs were inconclusive due to very small size of the cluster. TEM and XPS of Cu clusters was reported in the previous work [12], The TEM of the Cu clusters show that the clusters were in the 0.8-0.9 nm size range. The XPS analysis confirmed that the particles are only partially oxidised during deposition as both Cu^0 and Cu^+ signals were observed.

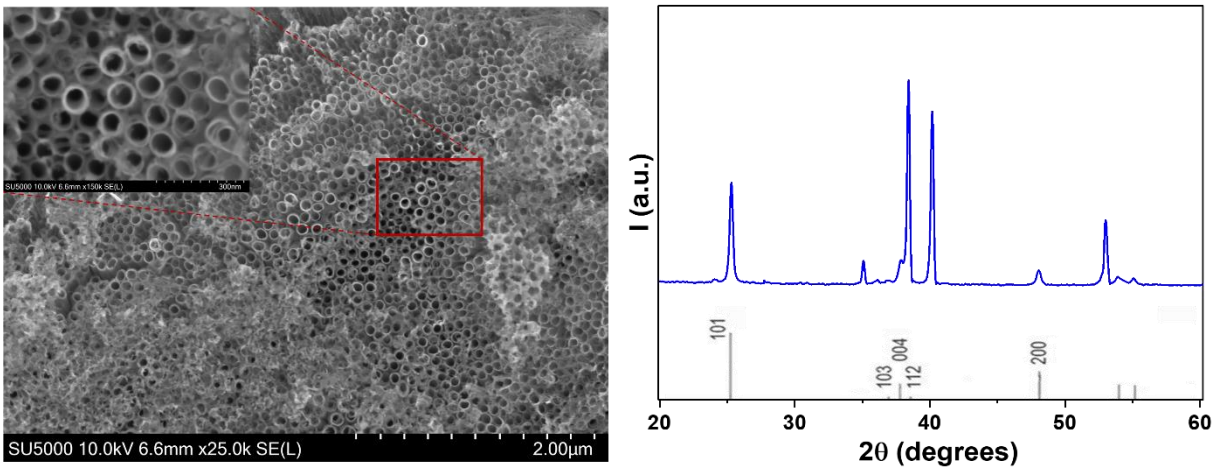

Fig. 1. (a) SEM image of the aligned titania nanotubes, (inset) zoomed-in to the selected area and (b) corresponding XRD pattern. Anatase spectra (JCPDS card no. 21-1272) is added for reference.

The TEM analysis (Fig. 2 (a,b)) of TiNTs shows that the nanotubes have an outer diameter in 50-60 nm range. The inner diameter of the nanotubes varies with the distance from the surface. The diameter at the open end is 27-30 nm and the diameter at the bottom is 17-20 nm. Due to the variation in the inner tube diameter, the nanotube wall thickness varies from 14-16 nm at the open end to 18-22 nm near the capped region. The lengths of the nanotubes are in 1.1-1.2 µm range. The inset in Fig. 2(a) shows the SAED pattern of the nanotubes indicates only the anatase phase. The TEM analysis of the side of the wall indicates that the nanotube walls have no preferential orientation.

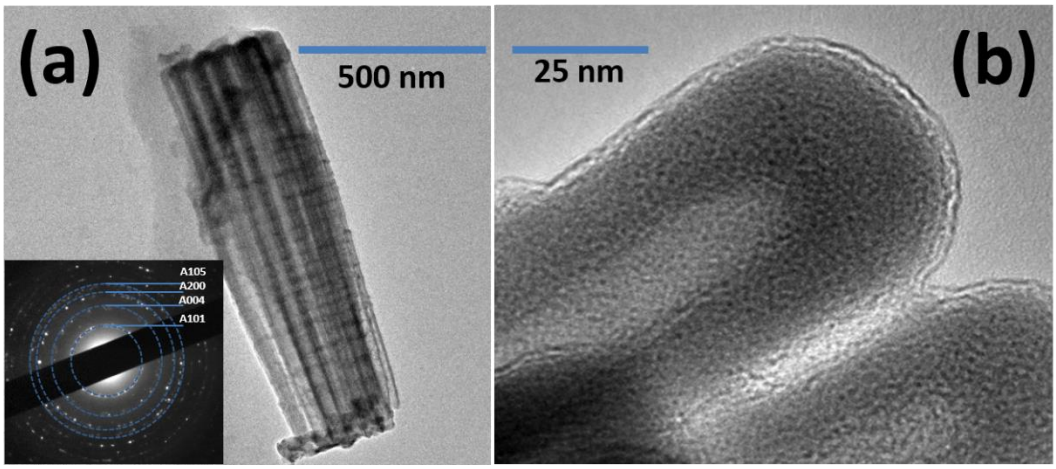

Fig. 2. (a) TEM and (b) HRTEM images of TiNTs. Inset (a) shows the SAED pattern of the TiNTs.

An effort was made to determine the copper cluster distribution on the TiNTs surface using TEM but due to very small size of the clusters, it was not possible to observe them. Further, STEM-HAADF and STEM-BF measurements were performed to get the copper distribution on the nanotubes surface including tube. As shown in figure 3, only few Cu clusters could be observed inside the tube. The size of the particles were approximately 2 nm which indicates the particles being a agglomeration of the primary particles. The primary clusters (size <1 nm) could not be observed in both TEM and STEM. In a previous report, Tavella *et al.* spray coated copper nanoparticles and the particles were uniformly distributed in the titania nanotubes [15]. As the clusters in the investigation were deposited using spray-coating, it is believed that the clusters were distributed on the TiNTs surface including the tube. The only difference

is that their copper particles were bigger in size (0.9 nm instead of 3nm). *Gharaei et al.* performed DFT calculations to indicate that only the centre inserted Cu supports the enhanced photocatalytic activity from Cu-TiNTs samples, further indicating Cu clusters presence in the tube [16].

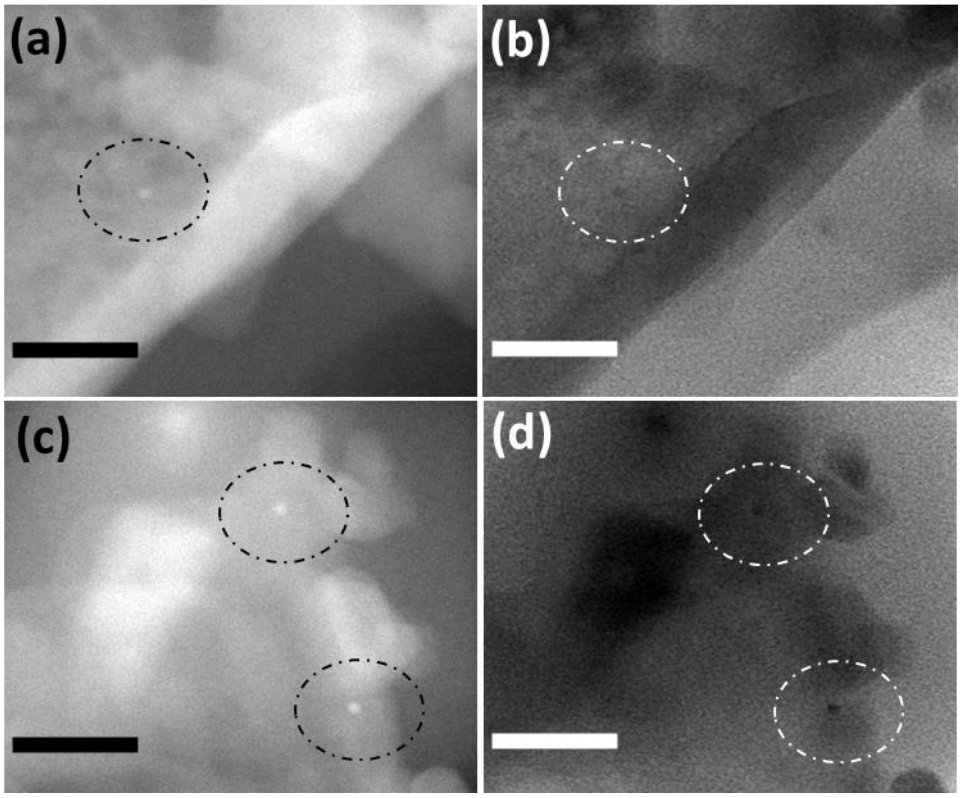

Fig. 3. (a,c) STEM-HAADF and (b,d) corresponding STEM-BF images of Cu-TiNTs post annealing. The circled spots which are there in both BF and DF images are the copper clusters. The scale bar in all the STEM images is 20 nm.

3.2. Photoelectrochemical responses

Photoelectrochemical characterisation comparing unmodified and Cu modified TiNTs showed the enhancement in the UV-Vis photocurrent response relative to the unmodified material. The results were shown from the optimised Cu loading on TiNTs surface. Fig. 4(a) shows the current – potential plot of TiNTs. The photocurrent magnitude at +0.65 V from TiNTs and Cu-TiNTs are 150 and 187 µA, respectively indicating an enhancement of 25%. The anodic onset potential or the flat band potential for TiNTs is -0.37 V vs SCE and for Cu-TiNTs is -0.23 V vs SCE. This indicates that the quasi-Fermi level (under irradiation) shifts slightly to a lower value, away from the conduction band, after the surface modification [17]. The Cu-TiNTs sample showed a small visible light (>435nm) induced photocurrent of 1.7 µA +0.65 V (Fig. 4(b)). The unmodified TiNTs showed no visible photocurrent. The visible photocurrent was less than 1% of the UV-Vis photocurrent.

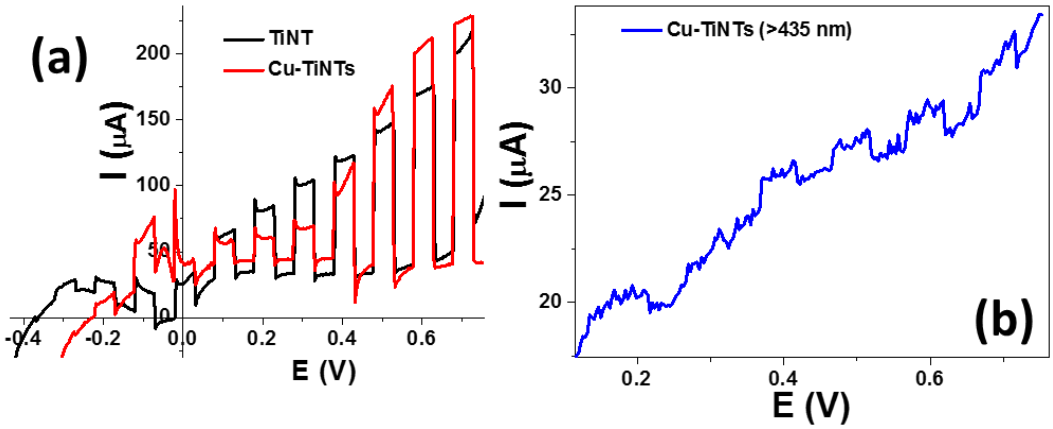

Fig. 4. (a) Chopped LSV of TiNTs before and after copper loading, and (b) LSV of Cu-TiNTs after application of 435 nm filter. Irradiation source 450 W Xe, electrolyte 0.1 M $HClO_4$, 5 mVs^{-1}, 10s exposure-dark cycle.

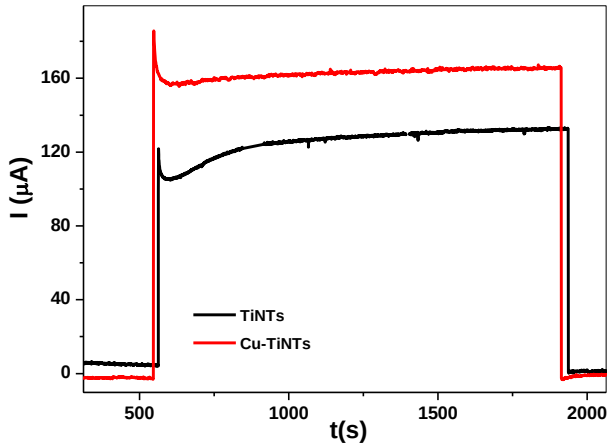

Fig. 5. Photocurrent at fixed potential of 0.5 V for TiNTs before and after copper loading. Irradiation source 450 W Xe, electrolyte 0.1 M $HClO_4$.

LSV sometimes may not provide an exact value of the photocurrent due to slow reaction kinetics and traps. Therefore, photocurrent measurements at fixed potential of 0.5 V were also carried out. As shown in Fig. 5, the TiNTs and Cu-TiNTs showed the steady-state photocurrent magnitudes of 133 and 170 μA, respectively. This is an enhancement of 28% in the photocurrent response from Cu-TiNTs as compared to the TiNTs. No visible photocurrent response was observed from the Cu modified electrodes at any fixed potential during monochromatic light measurements. This indicates that the visible response measured by LSV (Fig. 4(b)) from Cu-TiNTs is likely due to the surface traps.

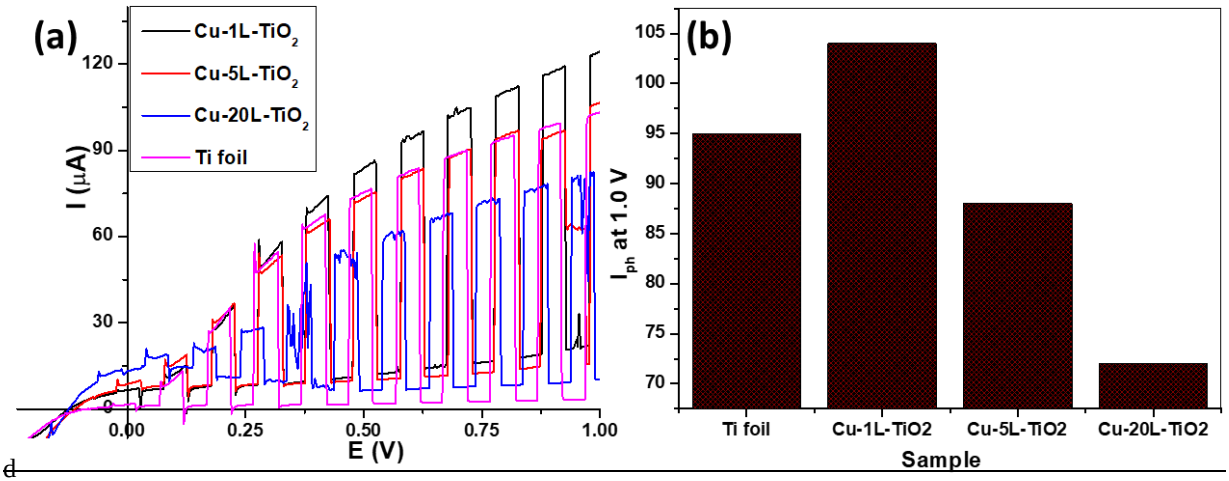

Fig. 6. (a) LSV for various loadings of Cu on TiO_2 foils at 5 mVs-1 sweep rate and 10 s exposure-delay cycle. (b) The photocurrent response at +1.0 V as a function of Cu loading on Ti foil.

The Cu cluster loading was optimised on titania films. Figure 6(a) shows the LSV response from the TiO_2 foils for different loadings of Cu clusters. Figure 6(b) shows the photocurrent response from the samples at 1.0 V. Cu-1L-TiO_2 corresponds to the theoretical monolayer of Cu cluster on TiO_2 surface, which is optimised. 5L and 20L correspond to five and twenty layers of Cu clusters. As shown in the figure 6(b), the further enhancement of the Cu cluster loading on TiO_2 reduces the photocatalytic activity. This can be due to either the enhancement of trap states at the surface or light shielding upon enhancement in Cu cluster loading.

To determine the photocurrent contribution from each of the wavelength, monochromatic photons were irradiated on the electrodes to obtain the photocurrent action spectra. Fig. 7 shows the photocurrent spectra for TiNTs and Cu-TiNTs samples. The measurements were carried out in the wavelength range of 280-440 nm range. The spectral response of the Cu-TiNTs enhanced at each wavelength as compared to TiNTs. The peak photocurrent response from both unmodified and modified NTs was obtained at 340 nm. The action spectra were used to obtain IPCE for both TiNTs and Cu-TiNTs. As seen in Fig. 8(a), the photocurrent enhances at each wavelength for TiNTs with Cu loading. As anatase is an indirect bandgap material, the plot of $(IPCE h\upsilon)^{1/2}$ vs photon energy ($h\upsilon$) is used for the bandgap determination similar to the diffused reflectance used for optical band-gap determination [18]. As shown in Fig. 8(b), there is no shift in the bandgap of TiNTs after Cu modification and both materials have 3.14 eV band-gap.

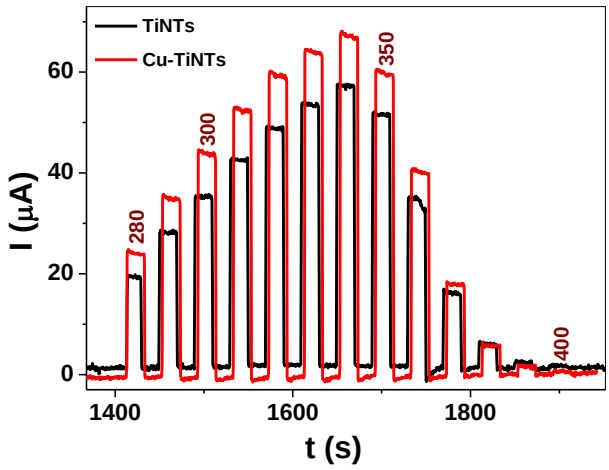

Fig. 7. Spectral response of TiNTs before and after copper loading at +0.5 V vs SCE. The number above each peak indicates the wavelength at which photocurrent is measured. Irradiation source 450 W Xe, electrolyte 0.1 M $HClO_4$, at 10 nm interval, 20 s exposure-delay cycle.

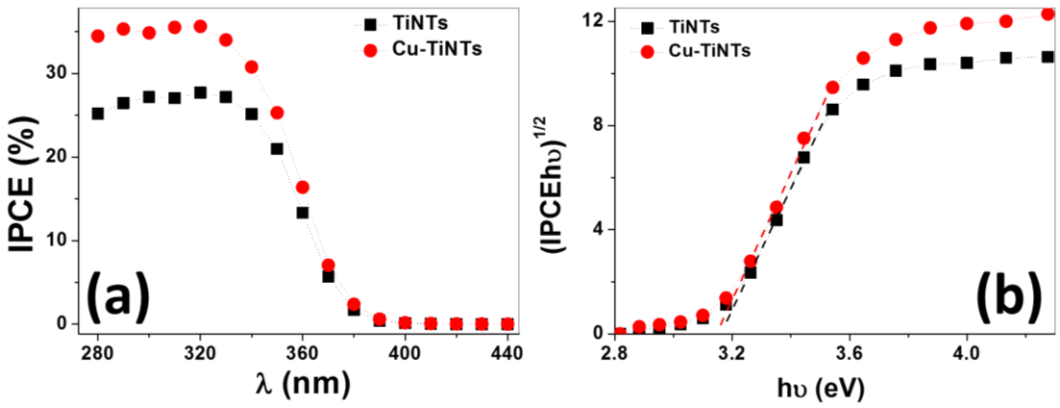

Fig. 8. (a) The IPCE% from TiNTs before and after copper loading plotted as a function of wavelength and (b) $(IPCEh\upsilon)^{1/2}$ as a function for photon energy for bandgap determination.

The increased photocurrent response at all wavelengths in UV region but no response in the visible region indicates that Cu modification did not dope a second energy level into the photocatalyst system to enhance activity. Additionally, a more positive onset potential upon the surface modification with copper indicates that the overpotential for the reductive reactions is reduced (Fermi level under irradiation shifting away from CB edge) [17]. The effective mass of the holes (m_h^*) is much higher than electrons holes (m_e^*). Both hole and electron transport across the interface, in opposite directions at comparable rates, are important for higher photocatalytic efficiency. Therefore, the effective charge separation is almost always limited by the hole transportation. The Cu clusters attached to the surface to enhance the photoresponse have previously been reported to provide better charge separation by scavenging holes (reducing their availability for recombination) and thereby providing a better charge separation pathway [19]. Therefore, in this investigation the surface modified samples demonstrate a higher photocurrent due to the enhanced separation of charge carriers and reduced recombination.

Other mechanisms of activity enhancement by surface modification such as by the removal of hole traps and, passivation of surface defects or Ti^{3+}, that are known recombination centres will require further study [19]. As the state of the art currently does not provide a simple method of eliminating these possibilities the mechanism of by which surface modification of clusters of copper enhanced UV response of the material is unknown. However, this study shows an example of the role of surface modifiers improving activity without doping or forming a second photoactive heterostructure.

4. Conclusions

Titania nanotubes were successfully fabricated on Ti foil using electrochemical anodization and it had anatase crystalline structure as shown by the SEM images and XRD. The nanotubes had a very good coverage on the surface. The nanotubes were loaded with synthesized Cu clusters and samples were investigated for their photoelectrochemical responses. The photocurrent magnitude of titania nanotubes enhanced upon loading with cu clusters as measured by LSV and photocurrent measurements at fixed potential. The photocurrent action spectrum depicts that the photocurrent enhancement is only in the UV response of the nanotubes, without any red-shift. IPCE was used to determine the band-gap and both the samples showed a band-gap of 3.14 eV. This study shows surface modifiers often reported to enhance photocatalytic activity can do so without changing the band gap of the parent material. However, further explorations of the changes in charge transfer due to the surface modifiers and the cluster distribution on the parent material is still needed to guide the development of surface modification process for improved photocatalysts.

Acknowledgements

PS would like to acknowledge Invest NI for biodevices project and Ulster University for the VCRS scholarship during his PhD.

References

[1] A. Kudo and Y. Miseki, Chem. Soc. Rev. 38 (2009) 253-278.

[2] A. Fujishima, X. Zhang and D.A. Tryk, Surf. Sci. Rep. 63 (2008) 515-582.

[3] M.R. Hoffman, S.T. Martin, W. Choi, D.W. Bahnemann, Chem. Rev. 95 (1995) 69-96.

[4] A. Linsebigler, G. Lu, J.T. Yates, Chem. Rev. 95 (1995) 735-58.

[5] J.A. Byrne, P.S.M. Dunlop, J.W.J. Hamilton, P. Fernández-Ibáñez, I. Polo-López, P.K. Sharma, A.S.M. Vennard, Molecules 20 (2015) 5574-5615.

[6] J. Cabrera, H. Alarcón, A. López, R. Candal, D. Acosta, J. Rodriguez, Water Sci. Technol. 70 (2014) 972–979.

[7] P. Roy, S. Berger, P. Schmuki, Angew. Chem. Int. Ed. 50 (2011) 2904 – 2939.

[8] K.C. Schwartzenberg, J.W.J. Hamilton, A.K. Lucid, E. Weitz, J. Notestein, M. Nolan, J.A. Byrne, K.A. Gray, Catal. Today 280 (2017) 65–73.

[9] J. Ohyama, A. Yamamoto, K. Teramura, T. Shishido and T. Tanaka, ACS Catal. 1 (2011) 187.

[10] Q. Jin, M. Fujishima, A. Iwaszuk, M. Nolan, H. Tada, J. Phys. Chem. C 117 (2013) 23848–23857.

[11] L.S. Yoong, F.K. Chong and B.K. Dutta, Energy 34 (2009) 1652–1661.

[12] P.K. Sharma, M.A. Cortes, J.W.J. Hamilton, Y. Han, J.A. Byrne, M. Nolan, Catal. Today 321 (2019) 9-17.

[13] C. Boyle, N. Skillen, H.Q.N. Gunaratne, P.K. Sharma, J.A. Byrne, P.K.J. Robertson, Mater. Sci. Semicond. Process. 109 (2020) 104930.

[14] Z.B. Chen, T.F. Jaramillo, T.G. Deutsch, A. Kleiman-Shwarsctein, A.J. Forman, N. Gaillard, R. Garland, K. Takanabe, C. Heske, M. Sunkara, E.W. McFarland, K. Domen, E.L. Miller, J.A. Turner, H.N. Dinh, J. Mater. Res. 2010, 25, 3–16.

[15] Tavella et al., Development of photoanodes for photoelectrocatalytic solar cells based on copper-based nanoparticles on titania thin films of vertically aligned nanotubes, Catalysis Today, 2018, 304, 190–198.

[16] Gharaei et al., Bandgap reduction of photocatalytic TiO2 nanotube by Cu doping, Scientific Reports, 2018, 8, 14192.

[17] K. Wang, T. Peng, Z. Wang, H. Wang, X Chen, W. Daia, Xianzhi Fu, Appl. Catal. B Environ. 250 (2019) 89–98.

[18] A. Mazare, I. Paramasivam, F. Schmidt-Stein, K. Lee, I. Demetrescu, P. Schmuki, Electrochim. Acta 66 (2012) 12–21.

[19] P. V. Kamat, J. Phys. Chem. Lett. 3 (2012) 663-672.